

Synthesis, Structure, and Reactivities of $[\eta^2\text{-P}_7\text{M}(\text{CO})_4]^{3-}$, $[\eta^2\text{-HP}_7\text{M}(\text{CO})_4]^{2-}$, and $[\eta^2\text{-RP}_7\text{M}(\text{CO})_4]^{2-}$ Zintl Ion Complexes Where M = Mo, W

Scott Charles, James C. Fettinger, and Bryan W. Eichhorn*

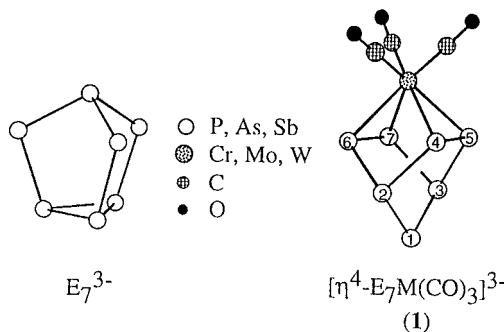
Department of Chemistry and Biochemistry, University of Maryland, College Park, Maryland 20742

Received August 29, 1995[⊗]

Ethylenediamine (en) solutions of $[\eta^4\text{-P}_7\text{M}(\text{CO})_3]^{3-}$ ions [M = W (**1a**), Mo (**1b**)] react under one atmosphere of CO to form microcrystalline yellow powders of $[\eta^2\text{-P}_7\text{M}(\text{CO})_4]^{3-}$ complexes [M = W (**4a**), Mo (**4b**)]. Compounds **4** are unstable, losing CO to re-form **1**, but are highly nucleophilic and basic. They are protonated with methanol in en solvent giving $[\eta^2\text{-HP}_7\text{M}(\text{CO})_4]^{2-}$ ions (**5**) and are alkylated with R_4N^+ salts in en solutions to give $[\eta^2\text{-RP}_7\text{M}(\text{CO})_4]^{2-}$ complexes (**6**) in good yields (R = alkyl). Compounds **5** and **6** can also be prepared by carbonylations of the $[\eta^4\text{-HP}_7\text{M}(\text{CO})_3]^{2-}$ (**3**) and $[\eta^4\text{-RP}_7\text{M}(\text{CO})_3]^{2-}$ (**2**) precursors, respectively. The carbonylations of **1–3** to form **4–6** require a change from η^4 - to η^2 -coordination of the P₇ cages in order to maintain 18-electron configurations at the metal centers. Comparative protonation/deprotonation studies show **4** to be more basic than **1**. The compounds were characterized by IR and ¹H, ¹³C, and ³¹P NMR spectroscopic studies and microanalysis where appropriate. The $[\text{K}(2,2,2\text{-crypt})]^+$ salts of **5** were characterized by single crystal X-ray diffraction. For **5**, the M–P bonds are very long (2.71(1) Å, average). The P₇³⁻ cages of **5** are not displaced by dppe. The P₇ cages in **4–6** have nortricyclane-like structures in contrast to the norbornadiene-type geometries observed for **1–3**. ³¹P NMR spectroscopic studies for **5–6** show C₁ symmetry in solution (seven inequivalent phosphorus nuclei), consistent with the structural studies for **5**, and C_s symmetry for **4** (five phosphorus nuclei in a 2:2:1:1:1 ratio). Crystallographic data for $[\text{K}(2,2,2\text{-crypt})]_2[\eta^2\text{-HP}_7\text{W}(\text{CO})_4]\cdot\text{en}$: monoclinic, space group C2/c, a = 23.067(20) Å, b = 12.6931(13) Å, c = 21.433(2) Å, β = 90.758(7)°, V = 6274.9(10) Å³, Z = 4, R(F) = 0.0573, R_w(F²) = 0.1409. For $[\text{K}(2,2,2\text{-crypt})]_2[\eta^2\text{-HP}_7\text{Mo}(\text{CO})_4]\cdot\text{en}$: monoclinic, space group C2/c, a = 22.848(2) Å, b = 12.528(2) Å, c = 21.460(2) Å, β = 91.412(12)°, V = 6140.9(12) Å³, Z = 4, R(F) = 0.0681, R_w(F²) = 0.1399.

Introduction

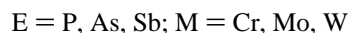
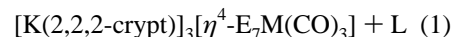
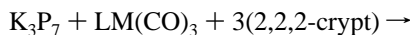
The chemistry of the soluble p-block polyanions (Zintl ions) with transition metal complexes is an emerging area of science. Although the first reports of naked Zintl ions are now over 100 years old,^{1–6} the chemistry of these compounds^{7,8} and, in particular, the first compounds containing Zintl ions bound to transition metals have only recently been reported.^{9–17} We have been investigating the chemistry of the E₇³⁻ Zintl ions (E = P, As, Sb) that have the nortricyclane-like structure. In recent papers, we and others have described the synthesis and



[⊗] Abstract published in *Advance ACS Abstracts*, February 15, 1996.

- (1) Joannis, A. C. *R. Hebd. Seances Acad. Sci.* **1891**, 113, 795.
- (2) Joannis, A. C. *R. Hebd. Seances Acad. Sci.* **1892**, 114, 585.
- (3) Kraus, C. A. *J. Am. Chem. Soc.* **1907**, 29, 1557.
- (4) Kraus, C. A. *J. Am. Chem. Soc.* **1922**, 44, 1216.
- (5) Zintl, E.; Harder, A. Z. *Phys. Chem. Abt. A* **1931**, 154, 47.
- (6) Zintl, E.; Goubeau, J.; Dullenkopf, W. Z. *Phys. Chem. Abt. A* **1931**, 154, 1.
- (7) von Schnering, H. G. *Angew. Chem., Int. Ed. Engl.* **1981**, 20, 33.
- (8) Corbett, J. D. *Chem. Rev.* **1985**, 85, 383.
- (9) Fritz, G.; Hoppe, K. D.; Hönl, W.; Weber, D.; Mujica, C.; Manriquez, V.; von Schnering, H. G. *J. Organomet. Chem.* **1983**, 249, 63.
- (10) von Schnering, H. G.; Wolf, J.; Weber, D.; Ramirez, R.; Meyer, T. *Angew. Chem., Int. Ed. Engl.* **1986**, 25, 353.
- (11) Eichhorn, B. W.; Haushalter, R. C.; Pennington, W. T. *J. Am. Chem. Soc.* **1988**, 110, 8704.
- (12) Eichhorn, B. W.; Haushalter, R. C.; Huffman, J. C. *Angew. Chem., Int. Ed. Engl.* **1989**, 28, 1032.
- (13) Eichhorn, B. W.; Haushalter, R. C. *J. Chem. Soc., Chem. Commun.* **1990**, 937.
- (14) Charles, S.; Eichhorn, B. W.; Bott, S. G. *J. Am. Chem. Soc.* **1993**, 115, 5837.
- (15) Fenske, D. *Abstracts of Papers*; 209th National Meeting of the American Chemical Society; Anaheim, CA, 1995; American Chemical Society: Washington, DC, 1995; INOR 299.
- (16) Teixidor, F.; Leutkens, M. L., Jr.; Rudolph, R. W. *J. Am. Chem. Soc.* **1983**, 105, 149.
- (17) Baudler, M.; Etzbach, T. *Angew. Chem., Int. Ed. Engl.* **1991**, 30, 580.

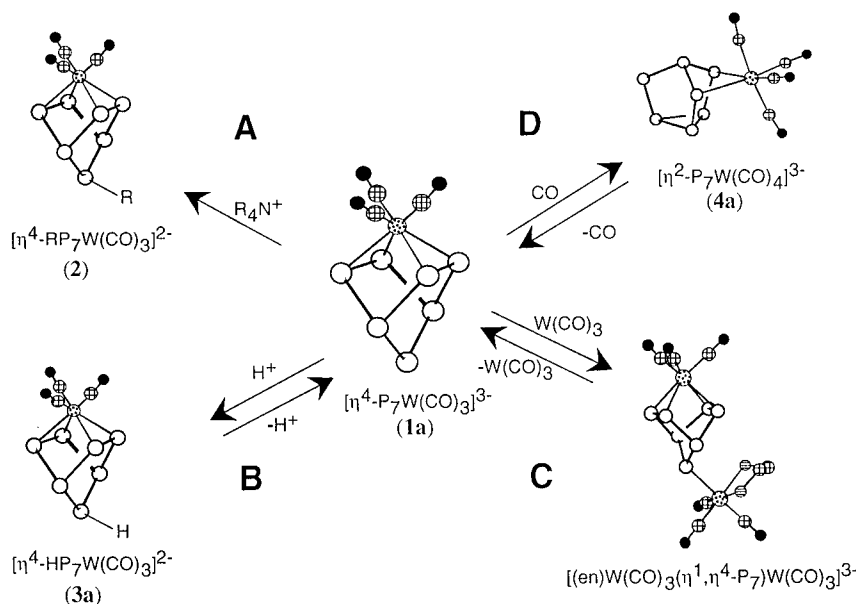
characterization of the $[\eta^4\text{-E}_7\text{M}(\text{CO})_3]^{3-}$ complexes (**1**), where E = P, As, Sb and M = Cr, Mo, W, in which the nortricyclane-like E₇³⁻ fragment is transformed into a norbornadiene-type fragment bound η^4 to the M(CO)₃ center.^{12,18,19} The reactions are accelerated by the use of 2,2,2-crypt “activators” that break the K⁺-E₇³⁻ ion pairing in solution and facilitate coordination of the E₇³⁻ ion to the transition metal center (eq 1).



Molecular orbital calculations of complexes **1** show high-lying pnictogen-based lone pairs that are localized on the E(1) site.^{18,19} It is not surprising, therefore, that electrophiles such as R⁺, H⁺, and W(CO)₃L_x react with these complexes at the E(1) site to form $[\eta^4\text{-XE}_7\text{M}(\text{CO})_3]^{n-}$ complexes (X = H, R,

- (18) Charles, S.; Bott, S. G.; Rheingold, A. L.; Eichhorn, B. W. *J. Am. Chem. Soc.* **1994**, 116, 8077.
- (19) Bolle, U.; Tremel, W. *J. Chem. Soc., Chem. Commun.* **1994**, 217.

Scheme 1

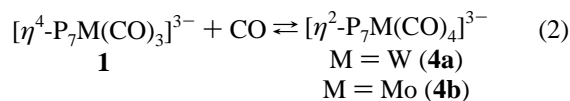


$\text{W}(\text{CO})_3$. Scheme 1 summarizes the reactions of $[\eta^4\text{-P}_7\text{W}(\text{CO})_3]^{3-}$ (**1a**) with various electrophiles (transformations A–C) and the nucleophile carbon monoxide (transformation D) as an example of the chemistry of the $[\eta^4\text{-E}_7\text{M}(\text{CO})_3]^{3-}$ complexes. The potent nucleophilicity of these compounds is unusual in that extremely weak electrophiles such as R_4N^+ ions serve as efficient alkylating agents in the formation of $[\eta^4\text{-RP}_7\text{W}(\text{CO})_3]^{2-}$ ions, (**2**), at room temperature (Scheme 1, transformation A).²⁰ In contrast to their high nucleophilicity, these compounds are only modestly basic. For example, $[\eta^4\text{-P}_7\text{W}(\text{CO})_3]^{3-}$ will deprotonate NH_4^+ but will *not* deprotonate MeOH in *en* or *dmf*. Its conjugate acid, $[\eta^4\text{-HP}_7\text{W}(\text{CO})_3]^{2-}$ (**3a**), is efficiently deprotonated by MeO^- in the same solvents (Scheme 1, transformation B).²¹

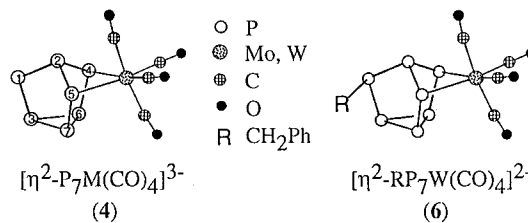
The transition metals in **1–3** have 18 valence electrons and are not susceptible to subsequent additions of Lewis bases under normal conditions. For example, **1–3** do not react with phosphines or amines and are in fact prepared in neat ethylenediamine solutions. However, under a carbon monoxide atmosphere, these compounds will reversibly bind a fourth CO ligand to form tetracarbonyl complexes (*i.e.* Scheme 1, transformation D). In these reactions, the P_7 ligand is driven from an η^4 - to an η^2 -coordination mode in order to accommodate the fourth CO ligand and maintain an 18 electron configuration at the transition metal center. In this paper, we report the synthesis, characterization, and interconversions of three types of tetracarbonyl complexes; namely $[\eta^2\text{-P}_7\text{M}(\text{CO})_4]^{3-}$ and $[\eta^2\text{-HP}_7\text{M}(\text{CO})_4]^{2-}$ complexes, where $\text{M} = \text{W}$ and Mo , and $[\eta^2\text{-RP}_7\text{W}(\text{CO})_4]^{2-}$, where $\text{R} = \text{alkyl}$.²² The formation of these compounds from the tricarbonyl precursors and their unusual trends in relative basicities, acidities, and stabilities are also described.

Results

Syntheses. Ethylenediamine (*en*) solutions of $[\eta^4\text{-P}_7\text{M}(\text{CO})_3]^{3-}$ ions [$\text{M} = \text{W}$ (**1a**), Mo (**1b**)] react under 1 atm of CO to form microcrystalline powders of $[\eta^2\text{-P}_7\text{M}(\text{CO})_4]^{3-}$ complexes in 71% ($\text{M} = \text{W}$) and ~18% ($\text{M} = \text{Mo}$) yields (eq 2) as the



$[\text{K}(2,2,2\text{-crypt})]^+$ salts. The $[\eta^2\text{-P}_7\text{M}(\text{CO})_4]^{3-}$ ions [$\text{M} = \text{W}$ (**4a**), Mo (**4b**)] are bright yellow and very air and moisture sensitive in solution and the solid state. Both compounds readily lose one CO ligand under N_2 atmospheres although the W complex **4a** is less prone to CO loss than **4b**. In addition, both compounds are more soluble but less stable in *dmf* than they are in *en*. Because of this instability, **4b** is always contaminated by **1b** impurities when under N_2 and low pressures of CO. Compounds **4** were characterized by IR, ^{13}C and ^{31}P NMR spectroscopic studies and microanalysis (**4a**). Although we were unable to obtain crystals suitable for a single crystal X-ray diffraction study, spectroscopic studies clearly indicate that complexes **4** contain an $\eta^2\text{-P}_7$ unit and C_s point symmetry.



Direct synthesis of **4a** from $\text{W}(\text{CO})_4(\text{py})_2$ and P_7^{3-} proceeds very slowly at room temperature according to eq 3 and is not an efficient synthetic route. Warming the solutions to accelerate the reactions affects a decarbonylation of the product to form **1a**. Reactions of $\text{Mo}(\text{CO})_4(\text{piperidine})_2$ and P_7^{3-} at room temperature do not give **4b** but yield instead mixtures of the protonated $[\eta^2\text{-HP}_7\text{Mo}(\text{CO})_4]^{2-}$ complex (**5b**) and the unprotonated tricarbonyl **1b** according to eq 4. The ratios of **5b** to **1b** obtained in eq 4 are dependent upon reaction conditions. Addition of $\text{Mo}(\text{CO})_4(\text{piperidine})_2$ to P_7^{3-} in hot *en* ($> \sim 70$

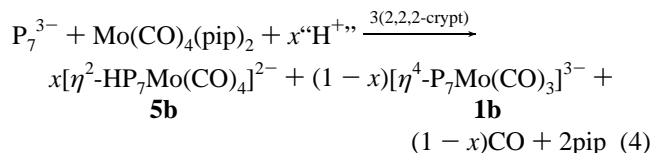
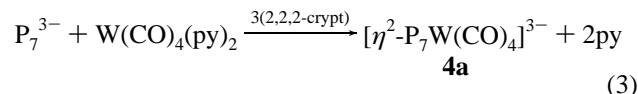
(20) Charles, S.; Fetting, J. C.; Eichhorn, B. W. *J. Am. Chem. Soc.* **1995**, *117*, 5303.

(21) Charles, S.; Eichhorn, B. W.; Fetting, J. C. Manuscript in preparation.

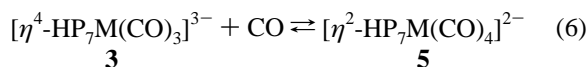
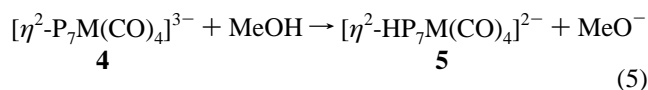
(22) The κ designations for all $\eta^4\text{-P}_7$ and $\eta^4\text{-XP}_7$ complexes ($\text{X} = \text{R}, \text{H}, \text{ML}_n$) described herein are $-\kappa\text{P}^4, \kappa\text{P}^5, \kappa\text{P}^6, \kappa\text{P}^7$ and refer to a common numbering scheme for the E_7 units used throughout this and previous^{18,20,23} publications. The kappa designations for all $\eta^2\text{-P}_7$ and $\eta^2\text{-XP}_7$ complexes ($\text{X} = \text{R}, \text{H}$) described herein are $-\kappa\text{P}^4, \kappa\text{P}^5$ and refer to the same common numbering scheme. For brevity, the κ designations have been omitted in text.

(23) Charles, S.; Eichhorn, B. W.; Bott, S. G.; Fetting, J. C. Submitted for publication.

°C) yields **1b** exclusively whereas room temperature reactions give ~ 5:1 ratios of **5b** to **1b**. The formation of **1b** formally involves a loss of CO from **4b** whereas **5b** is a protonation product of **4b**. The actual mechanisms of these reaction pathways and source of the proton are unknown at present. Proteo impurities in the solvent are unlikely proton sources in that pure unprotonated **1** and **4a** can be prepared under identical conditions.

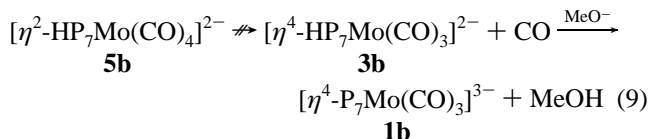
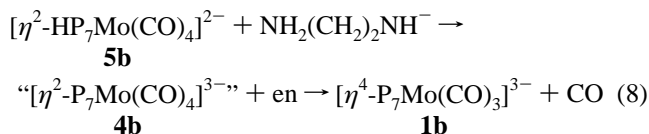
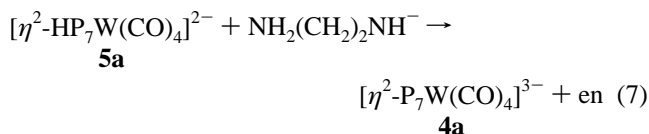


Compounds **5** are most conveniently prepared by direct protonation of **4** with methanol in en solvent (eq 5) but can also be prepared by carbonylation of the $[\eta^4-HP_7M(CO)_3]^{2-}$ ions (**3**) in en as shown in eq 6. Using eq 5 chemistry, **5a** can be



isolated as the $[K(2,2,2-crypt)]_2[\eta^2-HP_7W(CO)_4] \cdot en$ salt in 76% crystalline yield. Because of the lower solubility of **5b** relative to **1b**, eq 4 chemistry is the most convenient route for the preparation of $[K(2,2,2-crypt)]_2[\eta^2-HP_7Mo(CO)_4] \cdot en$ which was isolated in 40% crystalline yield using this method. The compounds are golden yellow in color and moderately air and moisture sensitive in solution and the solid state. As implied by the equilibrium shown in eq 6, **5a** and **5b** slowly lose one CO ligand under N₂ atmosphere in solution but are much more stable than **4**. Compounds **5** were characterized by microanalysis, IR and ¹H, ¹³C, and ³¹P NMR spectroscopic studies, and single crystal X-ray diffraction.

Unlike the tricarbonyl complexes **3** (see Scheme 1, transformation B), MeO⁻ is not a strong enough base to deprotonate **5** in en or dmf. However, **5a** is efficiently deprotonated by LiNH(CH₂)₂NH₂ in en to give **4a** according to eq 7. For **5b**,



deprotonation with LiNH(CH₂)₂NH₂ presumably gives **4b** as a transient intermediate, however **1b** is the only detectable product (eq 8). Identical experiments in which **5b** and excess NaOMe

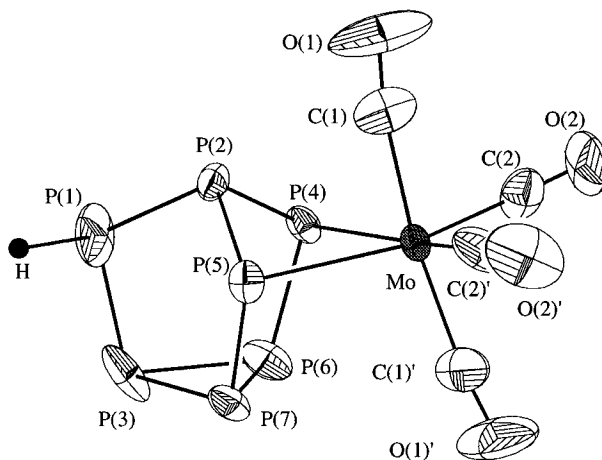
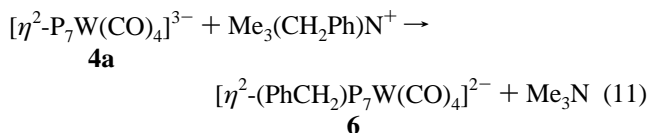
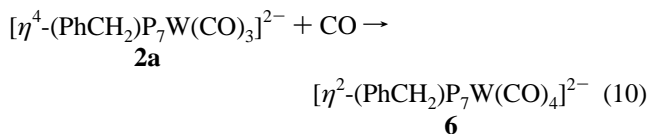


Figure 1. ORTEP drawing of the $[\eta^2-HP_7Mo(CO)_4]^{2-}$ ion (**5b**). The H atom was placed in an idealized position and was not located crystallographically.

(instead of LiNH(CH₂)₂NH₂) are stirred in en show unreacted **5b** after 48 h at room temperature. These experiments show that the **1b** formed by deprotonating **5b** with LiNH(CH₂)₂NH₂ proceeds through **4b** as outlined in eq 8 and not through **3b** as shown in eq 9. If **3b** were the intermediate in the formation of **1b**, the reaction with NaOMe would have been equally effective in the preparation of **1b** from **5b** (i.e. MeO⁻ readily deprotonates **3b**). In addition, the corresponding tungsten chemistry yields **4a** as an isolable intermediate in the deprotonation reactions.

Ethylenediamine solutions of $[\eta^4-(PhCH_2)_2P_7W(CO)_3]^{2-}$ (**2a**) react under an atmosphere of CO to form the yellow $[\eta^2-(PhCH_2)_2P_7W(CO)_4]^{2-}$ complex (**6**) according to eq 10. The reaction between Me₃(PhCH₂)N⁺ and $[\eta^2-P_7W(CO)_4]^{3-}$ also affords **6** according to eq 11. This reaction appears to proceed



faster ($t_\infty \leq 4$ h) than the alkylations reactions of **1a** ($t_\infty \approx 12$ h) at room temperature²⁰ (Scheme 1, path A), however, neither reaction rates were quantitatively measured. Through the use of eq 10 chemistry, transparent yellow crystals of **6** were isolated in 61% yield as the $[K(2,2,2-crypt)]_2[\eta^2-(PhCH_2)_2P_7W(CO)_4] \cdot en$ salt and have been characterized by microanalysis and IR and ¹H, ¹³C, and ³¹P NMR spectroscopic studies. Repeated attempts to grow X-ray quality crystals were unsuccessful, however, the spectroscopic studies show that **6** contains an η^2-P_7 unit (see below) and is isostructural to the protonated analog **5**. Carbonylations of other $[\eta^4-RP_7W(CO)_3]^{2-}$ complexes where R = Me, Et, and *n*-Bu²⁰ appear to proceed similarly but were not studied in detail.

Structural Studies. The $[K(2,2,2-crypt)]^+$ salts of the $[\eta^2-HP_7M(CO)_4]^{2-}$ complexes **5a** and **5b** are isotypic and crystallize in space group C2/c. An ORTEP drawing of **5b** is shown in Figure 1. A summary of the crystallographic data is given in Table 1 and a listing of selected bond distances and angles is given in Table 2.

The $[\eta^2-HP_7M(CO)_4]^{2-}$ ions have C₁ point symmetry due to the H atom on P(1) that destroys the mirror plane observed in

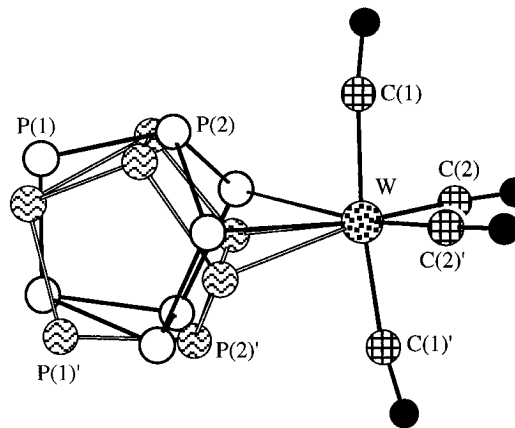
Table 1. Crystallographic Data for $[\text{K}(2,2,2\text{-crypt})]_2[\eta^2\text{-HP}_7\text{M}(\text{CO})_4]$ Where M = Mo, W

	M = Mo	M = W
formula	$\text{C}_{42}\text{H}_{81}\text{K}_2\text{MoN}_6\text{O}_{16}\text{P}_7$	$\text{C}_{42}\text{H}_{81}\text{K}_2\text{WN}_6\text{O}_{16}\text{P}_7$
fw	1317.10	1405.01
space group	$C2/c$	$C2/c$
a , Å	22.848(2)	23.067(20)
b , Å	12.528(2)	12.6931(13)
c , Å	21.460(2)	21.433(2)
α , deg	90	90
β , deg	91.412(12)	90.758(7)
γ , deg	90	90
V , Å ³	6140.9(12)	6274.9(10)
Z	4	4
cryst dimens, mm	$0.50 \times 0.20 \times 0.20$	$0.50 \times 0.20 \times 0.20$
cryst color	yellow	golden yellow
$D(\text{calcd})$, Mg/m ³	1.419	1.455
$\mu(\text{Mo K}\alpha)$, mm ⁻¹	0.595	0.395
temp, K	153(2)	293(2)
2θ scan range, deg	2.57–22.50	2.06–22.50
no. of reflns coll'd	4125	4478
no. of ind reflns	4008 [$R(\text{int}) = 0.0505$]	4096 [$R(\text{int}) = 0.0220$]
data/restraints/ params	4008/0/357	4096/0/363
no. of ind obsd reflns	2697	2833
$F_o > 4\sigma(F_o)$		
$R(F)^a$	0.0681	0.0573
$R_w(F^2)^b$	0.1399	0.1409
$\Delta/\sigma(\text{max})$	≤ 0.001	≤ 0.001
GOF	1.135	1.004

$$^a R(F) = \sum |F_o| - |F_c| / \sum F_o. \quad ^b R_w(F^2) = (\sum w(|F_o - F_c|)^2 / \sum w F_o^2)^{1/2}.$$

the $[\eta^2\text{-P}_7\text{M}(\text{CO})_4]^{3-}$ complexes. However, a 2-fold disorder of the P_7 group (see Figure 2) generates a crystallographic C_2 axis and $C2/c$ crystal symmetry. In one orientation, the P_7 cluster is positioned with P(2) "up" as illustrated in Figure 1 whereas the second orientation involves a 180° rotation of the P_7 cluster that leaves P(2)' "down" (Figure 2). The two orientations exist in a 1:1 ratio and share a common $\text{M}(\text{CO})_4$ fragment. The disorder was successfully modeled in both refinements. The P–H hydrogen is most likely disordered over four sites and was not located crystallographically.

In contrast to the $[\eta^4\text{-XP}_7\text{M}(\text{CO})_3]^{2-}$ complexes where X = H, R, $\text{M}(\text{CO})_3$, the $[\eta^2\text{-HP}_7\text{M}(\text{CO})_4]^{2-}$ structure type contains

**Figure 2.** Ball-and-stick representation of $[\eta^2\text{-HP}_7\text{W}(\text{CO})_4]^{2-}$ showing the orientational disorder of the HP_7 fragment in the crystal lattice.

a nortricyclane-like $\eta^2\text{-HP}_7$ fragment that is virtually unperturbed from the parent anion, P_7^{3-} . The metric parameters for **5a** and **5b** are virtually identical as illustrated in Table 2. The M–P bonds to P(4) and P(5) average 2.71 Å and are exceedingly long in comparison with typical M–P distances in related zerovalent carbonyl compounds which range between 2.4 and 2.5 Å.^{24,25} The length of the M–P bonds does not seem to indicate weak M–P interactions in that the clusters are not dissociating on the NMR time scale and are not displaced by en or dppe. The lack of correlation between M–P bond length and bond strength was recently described.²⁶ The M–P(6) and M–P(7) separations are clearly nonbonding (> 3.6 Å) which defines the η^2 coordination mode of the HP_7 unit. The P–P bonds range in length from 2.15 to 2.29 Å with the longest bonds located in the basal triangle defined by P(3), P(6), and P(7). The P(1)–P(2) bond of 2.09(2) Å in **5a** is anomalous and may be an artifact of the orientational disorder in the crystal. This range in bond lengths is similar to those of both the parent anion, P_7^{3-} , in Sr_3P_{14} (2.17–2.25 Å)²⁷ and $[\eta^4\text{-P}_7\text{Cr}(\text{CO})_3]^{3-}$ (2.114–2.237 Å).¹⁸

The M–C(1) distances (2.01(3) Å, average) of the mutually *trans* carbonyls are slightly longer than the M–C(2) distances (1.92(1) Å, average) due to the higher *trans* influence of CO relative to phosphorus ligands. The M–C(1) distances are typical

Table 2. Selected Bond Distances (Å) and Angles (deg) for the $[\eta^2\text{-HP}_7\text{M}(\text{CO})_4]^{2-}$ Ions

	M = Mo	M = W		M = Mo	M = W
Bonds					
M–C(1)	2.025(10)	2.000(13)	M–C(2)	1.919(10)	1.920(12)
C(1)–O(1)	1.141(10)	1.116(14)	C(2)–O(2)	1.173(10)	1.178(12)
M–P(4)	2.722(6)	2.691(11)	M–P(5)	2.717(6)	2.714(11)
P(1)–P(2)	2.15(2)	2.09(2)	P(1)–P(3)	2.190(12)	2.18(2)
P(2)–P(4)	2.148(8)	2.174(13)	P(2)–P(5)	2.180(8)	2.151(12)
P(3)–P(6)	2.24(2)	2.29(2)	P(3)–P(7)	2.25(2)	2.29(2)
P(4)–P(5)	3.268(8)	3.238(13)	P(4)–P(6)	2.175(7)	2.155(10)
P(5)–P(7)	2.169(7)	2.155(12)	P(6)–P(7)	2.195(7)	2.178(9)
Angles					
P(1)–P(2)–P(4)	99.2(5)	105.4(7)	P(1)–P(2)–P(5)	102.5(6)	100.8(7)
P(1)–P(3)–P(6)	99.3(10)	103.1(10)	P(1)–P(3)–P(7)	102.3(11)	100.1(10)
P(2)–P(1)–P(3)	103.7(12)	102.8(10)	P(2)–P(4)–P(6)	99.8(3)	99.3(5)
P(2)–P(5)–P(7)	99.8(3)	99.3(5)	P(3)–P(6)–P(4)	108.2(5)	106.3(6)
P(3)–P(6)–P(7)	60.9(4)	61.6(5)	P(3)–P(7)–P(5)	107.7(5)	105.9(6)
P(3)–P(7)–P(6)	60.6(4)	61.7(5)	P(4)–P(2)–P(5)	98.1(2)	97.0(3)
P(4)–P(6)–P(7)	104.3(2)	104.2(4)	P(5)–P(7)–P(6)	104.3(3)	104.3(4)
P(6)–P(3)–P(7)	58.5(4)	56.8(4)	P(2)–P(4)–M	81.8(2)	82.1(4)
P(2)–P(5)–M	81.4(2)	81.9(4)	P(4)–M–P(5)	73.86(12)	73.6(2)
P(4)–M–C(1)	83.6(3)	86.6(4)	P(4)–M–C(2)	169.6(3)	168.1(4)
P(5)–M–C(1)	86.6(3)	84.5(4)	P(5)–M–C(2)	169.1(3)	169.0(4)
P(6)–P(4)–M	96.8(2)	98.0(4)	P(7)–P(5)–M	96.6(3)	97.5(4)
C(1)–M–C(1)'	172.3(6)	172.6(8)	C(1)–M–C(2)	91.0(4)	91.3(5)
C(2)–M–C(2)'	87.7(5)	90.6(7)	M–C(1)–O(1)	171.6(11)	173(2)
M–C(2)–O(2)	178.8(9)	175.3(12)			

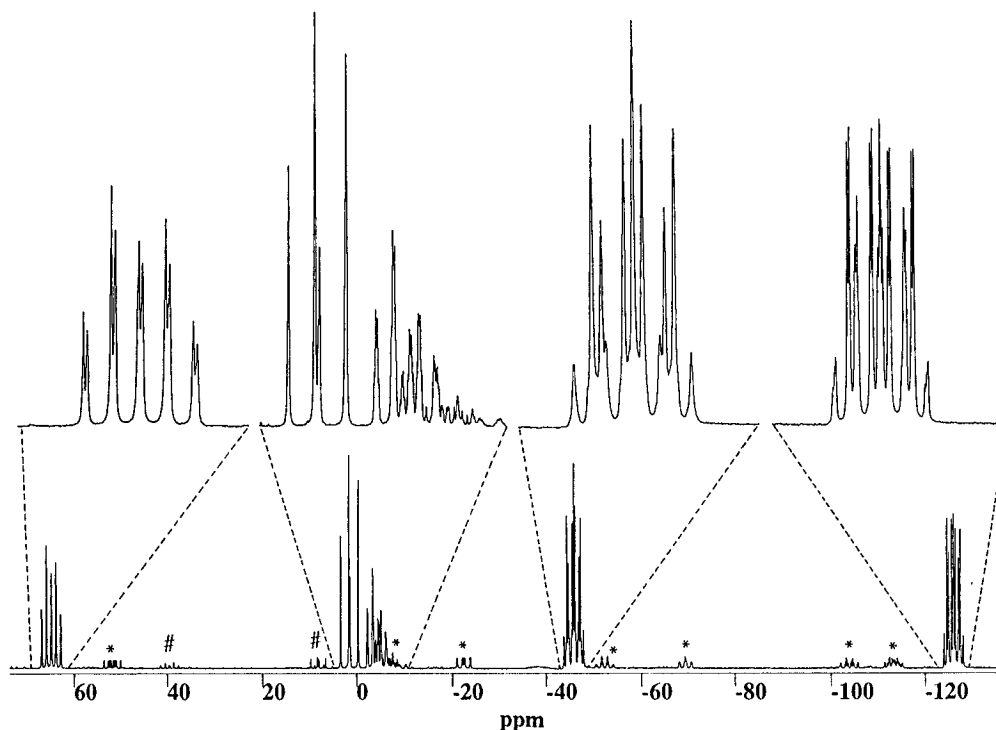


Figure 3. ^{31}P NMR spectrum of $[\eta^2\text{-P}_7\text{W}(\text{CO})_4]^{3-}$ (**4a**) recorded at 25 °C and 202 MHz in $\text{dmf-}d_7$ solution. The resonances marked with (*) arise from $[\eta^2\text{-HP}_7\text{W}(\text{CO})_4]^{2-}$ impurities. The resonances marked with (#) arise from an unidentified impurity.

for *trans* carbonyls on zerovalent tetracarbonyl complexes^{24,25} of Mo and W whereas the M–C(2) distances are somewhat shorter. The C(1) carbonyls are bent only slightly away from the HP_7 cage as evidenced by the C(1)–M–C(1') angles of 172.3(6)° for **5a** and 162.6(8)° for **5b**. Aside from the acute P(4)–M–P(5) angles of 73.7° (average) that result from the steric constraints of the HP_7 fragment, the geometry at the metal centers represent typical octahedra.

On the basis of the spectroscopic features of the $[\eta^2\text{-P}_7\text{M}(\text{CO})_4]^{2-}$ ions **4** (see below) and structural comparisons between **1**, **2**, and **5**, it is clear that **4** contains a $\eta^2\text{-P}_7$ fragment and C_s point symmetry. The mirror plane is defined by P(1), P(2), P(3), the transition metal, and the mutually *trans* carbonyl ligands as depicted in the schematic drawing shown previously.

The $[\eta^2\text{-(PhCH}_2)_7\text{P}_7\text{W}(\text{CO})_4]^{2-}$ ion **6** contains seven inequivalent phosphorus atoms as determined by ^{31}P NMR spectroscopic studies (see below) which is indicative of C_1 point symmetry. The spectroscopic similarities to **5** suggest the two are isostructural as implied by the schematic drawing of **6**.

NMR Spectroscopic Studies. The ^{31}P NMR spectra for the $[\eta^2\text{-P}_7\text{M}(\text{CO})_4]^{3-}$ ions **4** show five second-order resonances between +65 and –127 ppm of relative intensities 1:1:1:2:2 (see Figure 3) which is the basis for the proposed solid state structures. The mirror plane of the ion bisects two sets of phosphorus atoms, rendering them pairwise equivalent. On the basis of comparisons with related compounds, we propose the following assignments. The –127 and –46 ppm resonances of relative intensity two are assigned to the equivalent basal phosphorus atoms and the transition-metal-bound phosphorus atoms, respectively. The pseudotriplet-like character of the 3 ppm resonance is indicative of a two-coordinate phosphorus, and this resonance is assigned to P(1). The splitting patterns

of the 65 and –3 ppm resonances indicate that they arise from P(3) and P(2), respectively. The former resonance is unusual in that basal phosphorus resonances are typically found upfield of other resonances. The ^{13}C NMR spectrum of **4a** shows three resonances between 208 and 218 ppm in a 2:1:1 integral ratio, which is also consistent with the proposed structure. The downfield resonance of intensity two shows P–C coupling of 13 Hz whereas the upfield resonances appear as broad singlets. The ^{13}C chemical shifts are downfield of the $\text{W}(\text{CO})_6$ ($\delta = 192.1$ ppm) and upfield of **1a** ($\delta = 231.7$ ppm).

The ^{31}P NMR spectra for **5** show seven equal intensity resonances corresponding to the seven inequivalent phosphorus atoms observed in the solid state structure (see Figure 1). The 2-D ^{31}P – ^{31}P COSY NMR spectrum of **5b** is shown in Figure 4 as an example. In the proton-coupled ^{31}P NMR spectra, the resonance furthest downfield [35.5 ppm (**5a**), 49.5 ppm (**5b**)] shows $^1J_{\text{P-H}}$ coupling of 174 Hz, which is identical to that observed in the ^1H NMR spectra, and can therefore be assigned to P(1). Following this assignment, one can assign all seven resonances by way of 2-D ^{31}P – ^{31}P COSY NMR spectroscopy. Figure 4 shows a contour of the 2-D spectrum of **5b** in which only cross-peaks due to one-bond couplings are observed. Therefore, the two coordinate atoms P(1), P(4), and P(5) give resonances showing only two cross-peaks each whereas the other four phosphorus resonances show three cross-peaks. The peak labels shown in Figure 4 correspond to the labeling scheme used in Figure 1. The ^1H NMR spectrum of **5a** is shown in Figure 5. The P–H resonances for **5a** and **5b** appear as doublets of doublets of multiplets centered at 1.78 ppm. The resonance shows one-bond H–P coupling to P(1) of 174 Hz (average) and two-bond coupling to P(2) of 17 Hz. Additional couplings to the remaining phosphorus nuclei give rise to the multiplet patterns. The ^{13}C NMR spectra for **5** show four carbonyl resonances, three doublets and one singlet, due to the four inequivalent carbonyl ligands in the compounds. For both compounds, the two downfield doublets [214.2 and 213.8 ppm (**5a**); 222.9 and 222.3 ppm (**5b**)] show $^2J_{\text{P-C}}$ values of 7–10

(24) Sheldrick, W. S. *Chem. Ber.* **1975**, *108*, 2242.

(25) Atwood, J. L.; Darensbourg, D. J. *Inorg. Chem.* **1977**, *16*, 2314.

(26) Ernst, R. D.; Freeman, J. W.; Stahl, L.; Wilson, D. R.; Arif, A. M.; Nuber, B.; Ziegler, M. L. *J. Am. Chem. Soc.* **1995**, *117*, 5055.

(27) Dahlmann, W.; von Schnering, H. G. *Naturwissenschaften* **1972**, *59*, 420.

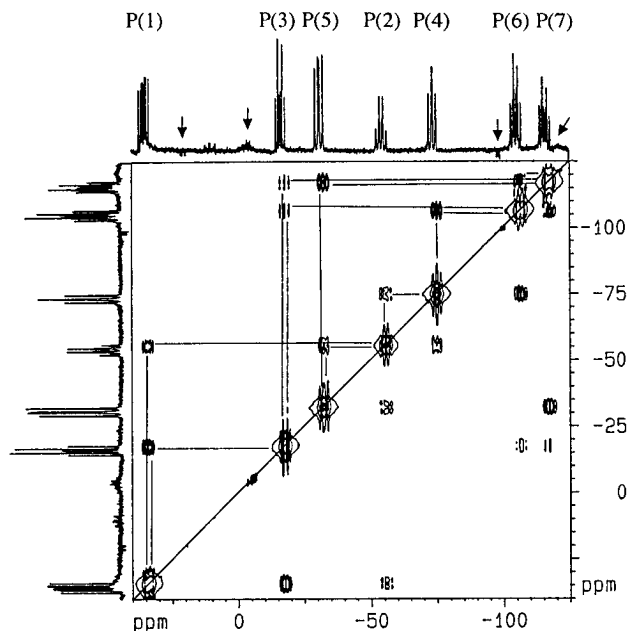


Figure 4. ^{31}P - ^{31}P COSY NMR spectrum for the $[\eta^2\text{-HP}_7\text{Mo}(\text{CO})_4]^{2-}$ ion (**5b**) recorded at 27 °C and 202 MHz from $\text{dmf-}d_7$ solution. The resonances marked with \downarrow arise from $[\eta^4\text{-HP}_7\text{Mo}(\text{CO})_3]^{2-}$ impurities.

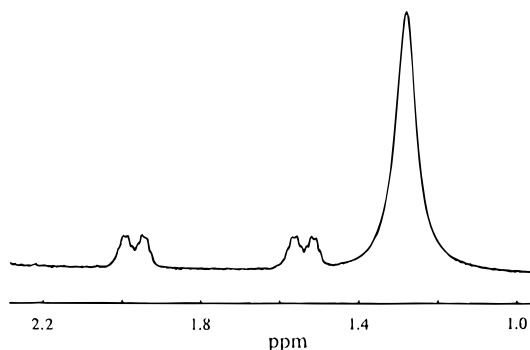


Figure 5. ^1H NMR spectrum for the $[\eta^2\text{-HP}_7\text{W}(\text{CO})_4]^{2-}$ ion (**5a**) recorded at 27 °C and 400 MHz from $\text{dmf-}d_7$ solution. The singlet at 1.3 ppm is associated with the en solvate molecule.

Hz. The upfield doublet [209.8 (**5a**), 214.9 (**5b**)] shows a larger $^2J_{\text{P-C}}$ value of 28.7 Hz. The fourth CO resonance is a broad singlet for both compounds with chemical shifts of 210.7 (**5a**) and 214.3 ppm (**5b**). The assignments and coupling constants were confirmed by recording the spectra at different spectrometer frequencies. The appearance of three *doublets* and one singlet for **5** indicates that the asymmetry imparted by the proton on the P_7 cage significantly affects the $^2J_{\text{P-C}}$ parameters.

The ^{31}P NMR spectrum for $[\eta^2\text{-(PhCH}_2)_7\text{P}_7\text{W}(\text{CO})_4]^{2-}$, **6**, contains seven equal intensity resonances between -119 and $+120$ ppm. Six of the seven resonances are within 14 ppm of the chemical shifts of $[\eta^2\text{-HP}_7\text{W}(\text{CO})_4]^{2-}$, **5a**, whereas the alkylated phosphorus P(1) resonance ($\delta = 120$ ppm) of **6** is shifted 70 ppm downfield of the corresponding protonated phosphorus resonance of **5a**. The carbonyl region of the ^{13}C NMR spectrum shows three doublets and a broad singlet between 215 and 210 ppm. The benzyl α -carbon resonance appears as a doublet at 26.9 ppm with $^2J_{\text{P-C}} = 30$ Hz. The peak positions, multiplicities, and general appearance of the ^{31}P and ^{13}C NMR spectra for **6** are quite similar to those of **5a** and are the basis for the similarities in proposed structures (see previous drawing). The ^1H NMR spectrum of **5a** shows resonances between 7.3 and 7.0 ppm due to the phenyl hydrogens of the benzyl group and “AB multiplets” at 1.83 and 1.53 ppm resulting from the diastereotopic benzyl α -hydrogens.

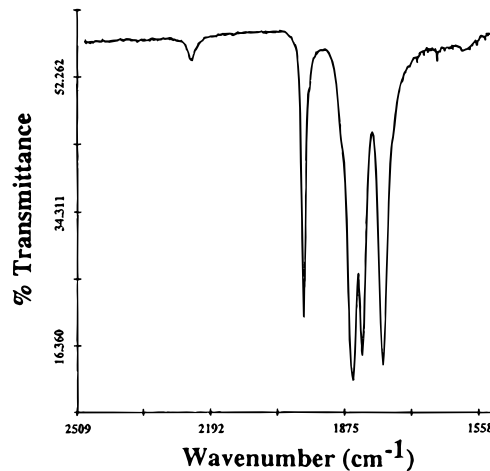
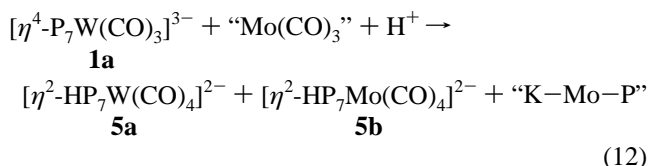


Figure 6. Solid-state IR spectrum (KBr pellet) showing the P-H and carbonyl regions of the $[\eta^2\text{-HP}_7\text{Mo}(\text{CO})_4]^{2-}$ ion (**5b**).

IR Spectroscopic Studies. The IR spectra (KBr pellet) for **4** show four $\nu(\text{CO})$ bands between 1940 and 1743 cm^{-1} whereas **5** and **6** show four bands between 1969 and 1778 cm^{-1} . These ranges are red-shifted from the related neutral $\text{L}_2\text{M}(\text{CO})_4$ complexes ($\text{L} = \text{phosphine}$) which range 2020–1870 cm^{-1} .^{28,29} Compounds **5** also show $\nu(\text{PH})$ modes at 2239 cm^{-1} . The $\nu(\text{PH})$ and $\nu(\text{CO})$ regions of **5b** are shown in Figure 6 as an example.

Discussion

Our initial discovery of the $[\eta^2\text{-HP}_7\text{M}(\text{CO})_4]^{2-}$ complexes **5** involved an attempted $\text{Mo}(\text{CO})_3/\text{W}(\text{CO})_3$ exchange reaction between $[\eta^4\text{-P}_7\text{W}(\text{CO})_3]^{3-}$ and (cycloheptatriene) $\text{Mo}(\text{CO})_3$. Although no exchange occurred in the absence of proteo impurities after several days,¹⁸ in the presence of H^+ the $[\text{K}(2,2,2\text{-crypt})]^+$ salts of $[\eta^2\text{-HP}_7\text{Mo}(\text{CO})_4]^{2-}$ and $[\eta^2\text{-HP}_7\text{W}(\text{CO})_4]^{2-}$ were isolated as well as an ill-defined “K-Mo-P” solid state compound³⁰ with a BaVS_3 ³¹ related structure (eq 12). While



this reaction is quite reproducible, it gives inseparable mixtures of products thus prompting us to develop the rational routes to the complexes described herein.

The general interconversions of **1**, **3**, **4**, and **5** are summarized in Scheme 2. Both of the carbonylation reactions involve the addition of a CO ligand to 18-electron, formally zerovalent metal centers. In order to facilitate the extra CO ligand, the P_7 groups change from a 6-electron-donor η^4 -coordination mode to a 4-electron-donor η^2 -coordination mode. Like **1–3**, complexes **5** and **6** are isolable and relatively stable toward CO loss in solution and the solid state. In contrast, compounds **4** readily lose CO under N_2 atmosphere, and only the tungsten complex **4a** has been prepared in a pure form.

For eq 2 chemistry, the reverse reaction is favored entropically, which could account for the general trend of decreased relative stability toward CO loss for the tetracarbonyl complexes

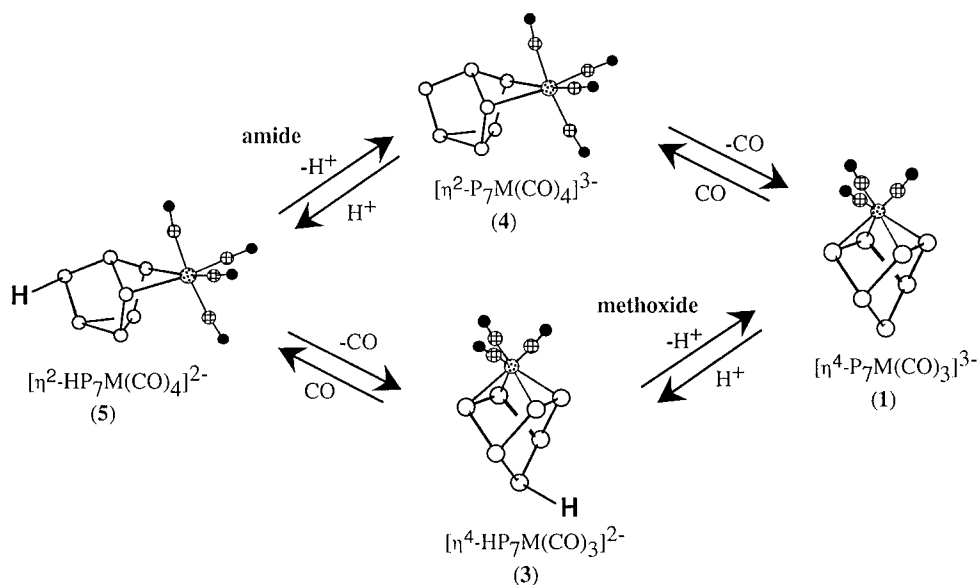
(28) Grim, S. O.; Briggs, W. L.; Barth, R. C.; Tolman, C. A.; Jesson, J. P. *Inorg. Chem.* **1974**, *13*, 1095.

(29) Darensbourg, D. J.; Kump, R. L. *Inorg. Chem.* **1978**, *17*, 2680.

(30) Charles, S.; Fetting, J. C.; Eichhorn, B. W. Results to be published.

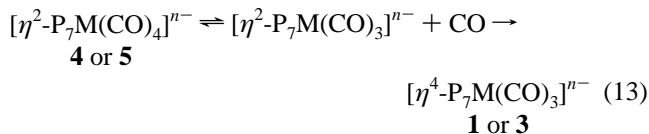
(31) Eichhorn, B. W. In *Progress in Inorganic Chemistry*; Karlin, K. D., Ed.; John Wiley & Sons: 1994; pp 139.

Scheme 2



relative to their tricarbonyl counterparts. However, the enhanced relative stability of the protonated tetracarbonyl complexes **5** in comparison to the unprotonated complexes **4** is somewhat curious. Upon protonation of the P₇ cage, the C–O bond strengths increase (higher ν_{CO}) which is usually accompanied by a decrease in the M–C bond strengths. However, the protonated compounds **5** are less prone to CO loss than **4**. These relative stabilities are consistent with the following two scenarios:

(1) If the tetracarbonyl complexes (**4** or **5**) rapidly (and reversibly) lose CO to give $\eta^2\text{-P}_7\text{M}(\text{CO})_3$ 16-electron intermediates, two reaction pathways can be envisaged and are shown in eq 13. The intermediate can either coordinate CO to reform the



tetracarbonyl complexes (no net reaction) or undergo a haptatropic shift of the P₇ ligand ($\eta^2 \rightarrow \eta^4$) to form the stable tricarbonyl compounds (**1** or **3**). Partitioning of products in eq 13 results from a competition between CO and the P₇ cage for the vacant coordination site at the 16-electron intermediate. The unprotonated P₇ cage of **4** is more nucleophilic and competes more effectively with CO than does the protonated HP₇ cage of **5**. The result is that the net loss of CO is faster for **4** than **5**.

(2) Alternatively, the haptatropic shift could be part of a concerted nucleophilic displacement of a CO ligand to form the tricarbonyl complexes without pre-dissociation of CO. In this case, the relative nucleophilicities of the protonated vs unprotonated P₇ cages would still give rise to the same relative stabilities of **4** vs **5**.

In either scenario, the unprotonated P₇³⁻ ligand of **4** is more nucleophilic than the protonated HP₇²⁻ cage of **5** and will favor formation of the tricarbonyl complexes (CO loss).

The series of compounds also show unusual trends in basicity and nucleophilicity. For example, addition of a CO ligand to **1** in the formation of **4** increases the basicity and nucleophilicity of the coordinated P₇ cage. These enhancements are evidenced qualitatively by the faster alkylation reactions of **4** (i.e. eq 11) relative to **1** (i.e. transformation A, Scheme 1) and quantitatively

in the acid–base reactions outlined in Scheme 2. Protonation of **4** in en solutions is easily accomplished using MeOH (eq 4) and the deprotonation of **5** requires a stronger base than MeO⁻ (i.e. an amide, eq 7). In contrast, protonation of **1** requires stronger acids than MeOH (i.e. HR₃N⁺ ions) to form **3**, and subsequent deprotonations are accomplished using MeO⁻ (see Scheme 2).²¹ The enhanced basicity and nucleophilicity of **4** can be understood through the following considerations. First, the P₇³⁻ ligand is functioning as a four-electron donor in **4** vs a six-electron donor in **1**; thus the metal does not require as much electron density from the P₇³⁻ fragment in **4** relative to **1**. Second, the molecular orbital calculations indicate a large degree of charge transfer from the P₇³⁻ ligand to the M(CO)₃ fragments in the electronic structure of **1**. In a limiting valence bond model for **1**, one could partition the charge in the form P₇³⁻--M(CO)₃²⁻ thus making it electronically equivalent to Fe(CO)₃(norbornadiene)³² and adequately describing the $\nu(\text{CO})$ energies. In contrast, the IR data for **4** show a lesser overall charge transfer suggesting a limiting valence bond description of P₇³⁻--M(CO)₄. Both of these factors could lead to enhanced basicity and nucleophilicity of the P₇ cage in **4** relative to **1**.

Finally, it is of interest to note that Bolle and Tremel have investigated similar reactions between Sb₇³⁻ and Mo(CO)₄(bipy) which gave low yields of Sb₁₁³⁻ and $[\eta^4\text{-Sb}_7\text{Mo}(\text{CO})_3]^{3-}$.^{19,33} Formation of the latter compound most likely proceeds through an unstable $[\eta^2\text{-Sb}_7\text{Mo}(\text{CO})_4]^{3-}$ intermediate similar to **4**. Our attempts to isolate this intermediate and the $[\eta^2\text{-Sb}_7\text{W}(\text{CO})_4]^{3-}$ analog are in progress.

Experimental Section

General Data. General operating procedures used in our laboratory have been described elsewhere.¹⁸ Proton (¹H) NMR spectra were recorded at ambient temperature on a Bruker AM400 (400.136 MHz) spectrometer. Carbon (¹³C) NMR spectra were recorded at ambient temperature on Bruker AF200 (50.324 MHz) and Bruker AM400 (100.614 MHz) spectrometers. Some of the ¹³C NMR chemical shifts and couplings were confirmed by recording the spectra at different magnetic field strengths. Phosphorus (³¹P) NMR spectra were recorded on Bruker WP200 (81.015 MHz) and AMX500 (202.458 MHz) spectrometers. The ³¹P–³¹P COSY NMR experiment was conducted on an AMX500.

(32) Albright, T. A.; Burdett, J. K.; Whangbo, M.-H. *Orbital Interactions in Chemistry*; John Wiley & Son, Inc.: New York, 1985, pp 218.

(33) Bolle, U.; Tremel, W. *J. Chem. Soc., Chem. Commun.* **1992**, 91.

The following is a list of observed data common to all compounds containing $[\text{K}(2,2,2\text{-crypt})]^+$. IR (KBr pellet), cm^{-1} : 3126 (m), 2957 (m), 2885 (m), 2817 (m), 1655 (m), 1597 (w), 1476 (m), 1459 (m), 1444 (m), 1400 (m), 1387 (s), 1362 (s), 1354 (s), 1299 (m), 1260 (m), 1238 (w), 1173 (w), 1132 (s), 1103 (s), 1081 (s), 1059 (m), 1030 (w), 950 (m), 933 (m), 830 (m), 820 (w), 806 (m), 754 (w), 667 (m), 638 (w), 614 (w), 572 (w), 546 (w), 525 (w). ^1H NMR (dmf- d_7), δ (ppm): 3.61 (s, 2,2,2-crypt), 3.58 (t, 2,2,2-crypt), 2.57 (t, 2,2,2-crypt), 2.54 (s, en), 1.26 (bs, en). $^{13}\text{C}\{^1\text{H}\}$ NMR (dmf- d_7), δ (ppm): 70.97 (s, 2,2,2-crypt), 68.34 (s, 2,2,2-crypt), 54.56 (s, 2,2,2-crypt), 46.28 (s, en).

Chemicals. The preparation of the K_3P_7 has been previously reported.¹⁸ **Caution!** Alkali metal polyphosphorus compounds are known to spontaneously detonate even under rigorously anaerobic conditions.³⁴ These materials should only be prepared in small quantities and should be handled with caution. (Cycloheptatriene)-molybdenum tricarbonyl, (mesitylene)tungsten tricarbonyl, tetracarbonylbis(piperidine)molybdenum, benzyltrimethylammonium bromide, and 4,7,13,16,21,24-hexaoxa-1,10-diazabicyclo[8.8.8]hexacosane (2,2,2-crypt) were purchased from Aldrich and used without further purification. Ethylenediamine (en) was purchased from Fisher (Anhydrous), distilled several times from CaH_2 under N_2 and then from K_4Sn_9 at reduced pressure, and finally stored under N_2 . Dimethylformamide (dmf) was purchased from Burdick & Jackson (High Purity), degassed, distilled at reduced pressure from K_4Sn_9 , and stored under N_2 . Carbon monoxide (CO) was purchased from Air Products and used without further purification. dmf- d_7 was purchased from Cambridge Isotope Laboratories and used without further purification. The preparation of $[\text{K}(2,2,2\text{-crypt})]_3[\eta^4\text{-P}_7\text{M}(\text{CO})_3]\cdot\text{en}$ ($\text{M} = \text{Mo}, \text{W}$) and $[\text{K}(2,2,2\text{-crypt})]_2[\eta^4\text{-(CH}_2\text{Ph)P}_7\text{W}(\text{CO})_3]\cdot\text{en}$ have previously been reported.^{18,20}

Syntheses. Preparation of $[\text{K}(2,2,2\text{-crypt})]_3[\eta^2\text{-P}_7\text{Mo}(\text{CO})_4]\cdot\text{en}$. In a 25 mL Schlenk flask, crystalline $[\text{K}(2,2,2\text{-crypt})]_3[\eta^4\text{-P}_7\text{Mo}(\text{CO})_3]\cdot\text{en}$ (114 mg, 0.067 mmol) was dissolved in en (~ 3 mL) yielding a red solution. The head gases were removed under vacuum and the flask back filled with CO (~ 1 atm). The flask was left open to the bubbler with a flow of CO for 30 s. The reaction mixture was vigorously stirred under a CO atmosphere for 12 h producing a yellow-orange solution and yellow-orange powder. The mother liquor was removed, the yellow-orange powder washed with tol and dried under vacuum (powder yield, 57 mg). IR spectroscopic analysis of the powder showed **5b** contaminates and ^{31}P NMR spectroscopic analysis of the mother liquor showed both **1b** and **5b** contaminates. IR data (KBr pellet), cm^{-1} : 1943 (s), 1830 (s), 1799 (s), 1748 (s). ^{31}P NMR (dmf- d_7), δ (ppm): 60 (m, 1 P), -11 (dd, 1 P), -16 (m, 1 P), -53 (m, 2 P), -130 (m, 2 P).

Preparation of $[\text{K}(2,2,2\text{-crypt})]_3[\eta^2\text{-P}_7\text{W}(\text{CO})_4]\cdot\text{en}$. In a 25 mL Schlenk flask, K_3P_7 (29.6 mg, 0.089 mmol), 2,2,2-crypt (100.0 mg, 0.27 mmol) and $(\text{C}_6\text{H}_3\text{Me}_3)\text{W}(\text{CO})_3$ (34.4 mg, 0.089 mmol) were combined in en (~ 3 mL). The reaction mixture was stirred for 12 h yielding a red solution. The head gases were removed under vacuum and the flask backfilled with CO (~ 1 atm). The flask was left open to the bubbler with a flow of CO for 30 s. The reaction mixture was vigorously stirred under a CO atmosphere for 12 h, producing a yellow solution and yellow powder. The mother liquor was removed and the yellow powder washed with tol and dried under vacuum (powder yield, 115 mg, 71%). Anal. Calcd for $\text{C}_{60}\text{H}_{116}\text{N}_8\text{O}_{22}\text{K}_3\text{P}_7\text{W}$: C, 39.61; H, 6.43; N, 6.16. Found: C, 39.79; H, 6.25; N, 6.31. IR data (KBr pellet), cm^{-1} : 1939 (s), 1819 (s), 1793 (s), 1744 (s). $^{13}\text{C}\{^1\text{H}\}$ NMR (dmf- d_7), δ (ppm): 218.1 (d, $J(\text{C},\text{P}) = 13$ Hz, CO), 214.5 (br s, CO), 211.6 (br s, CO). ^{31}P NMR (dmf- d_7), δ (ppm): 65 (m, 1 P), 3 (dd, 1 P), -3 (m, 1 P), -46 (m, 2 P), -127 (m, 2 P).

Preparation of $[\text{K}(2,2,2\text{-crypt})]_2[\eta^2\text{-HP}_7\text{Mo}(\text{CO})_4]\cdot\text{en}$. In a vial in a drybox, K_3P_7 (29.6 mg, 0.089 mmol), 2,2,2-crypt (100.0 mg, 0.27 mmol), and $(\text{C}_5\text{H}_{10}\text{NH})_2\text{Mo}(\text{CO})_4$ (33.7 mg, 0.089 mmol) were dissolved in en (~ 2 mL) and gently stirred for 3 h, yielding a red-orange solution. The reaction mixture was filtered through *ca.* one quarter inch of tightly packed glass wool in a pipet. After 24 h, the reaction vessel contained rectangular yellow-orange crystals that were removed from the mother liquor, washed with toluene, and dried under vacuum (crystalline yield, 47 mg, 40%). Anal. Calcd for $\text{C}_{42}\text{H}_{81}\text{N}_6\text{O}_{16}\text{K}_2\text{P}_7\text{Mo}$: C, 38.30; H, 6.20; N, 6.38. Found: C, 37.42; H, 5.89; N, 6.07. IR data (KBr pellet),

cm^{-1} : 2238 (w), 1969 (s), 1854 (s), 1831 (s), 1783 (s). ^1H NMR (dmf- d_7), δ (ppm): 1.78 (ddm, $^1J(\text{H},\text{P}) = 172$ Hz, $^2J(\text{H},\text{P}) = 16.7$ Hz). $^{13}\text{C}\{^1\text{H}\}$ NMR (dmf- d_7), δ (ppm): 222.9 (d, $^2J(\text{C},\text{P}) = 11$ Hz, CO), 222.3 (d, $^2J(\text{C},\text{P}) = 10$ Hz, CO), 214.9 (d, $^2J(\text{C},\text{P}) = 28.7$ Hz, CO), 214.3 (br s, CO). $^{31}\text{P}\{^1\text{H}\}$ NMR (dmf- d_7), δ (ppm): 35.5 (m, 1 P), -18.5 (m, 1 P), -31.5 (m, 1 P), -55.0 (m, 1 P), -74.0 (m, 1 P), -106.0 (m, 1 P), -118.0 (m, 1 P).

Preparation of $[\text{K}(2,2,2\text{-crypt})]_2[\eta^2\text{-HP}_7\text{W}(\text{CO})_4]\cdot\text{en}$. Method A. In a 25 mL Schlenk flask, 0.089 mmol of $[\text{K}(2,2,2\text{-crypt})]_3[\eta^2\text{-P}_7\text{W}(\text{CO})_4]\cdot\text{en}$ were generated *in situ* as described above (Method A). The powder was not isolated from the mother liquor. Instead, methanol (10 μL) was added under a flow of CO and the mixture stirred vigorously for 8 h under a CO atmosphere. The color of the solution remained yellow. After stirring, the mother liquor was removed leaving a yellow, powdery solid that was washed with toluene and dried under vacuum (powder yield, 96 mg, 76%).

Method B. In a 25 mL Schlenk flask, crystalline $[\text{K}(2,2,2\text{-crypt})]_2[\eta^4\text{-HP}_7\text{W}(\text{CO})_3]\cdot\text{en}$ (41 mg, 0.031 mmol) was dissolved in en (~ 2 mL) yielding a dark red solution. The head gases were removed under vacuum and the flask back filled with CO (~ 1 atm). The flask was left open to the bubbler with a flow of CO for 30 s. The reaction mixture was vigorously stirred under a CO atmosphere for 12 h, producing a yellow solution and yellow powder. ^{31}P NMR spectroscopic analysis of the mother liquor showed quantitative yield of **3b**. Anal. Calcd for $\text{C}_{42}\text{H}_{81}\text{N}_6\text{O}_{16}\text{K}_2\text{P}_7\text{W}$: C, 35.91; H, 5.81; N, 5.98. Found: C, 35.37; H, 5.64; N, 5.96. IR data (KBr pellet), cm^{-1} : 2240 (w), 1964 (s), 1843 (s), 1825 (s), 1778 (s). ^1H NMR (dmf- d_7), δ (ppm): 1.78 (ddm, $^1J(\text{H},\text{P}) = 172$ Hz, $^2J(\text{H},\text{P}) = 16.7$ Hz). $^{13}\text{C}\{^1\text{H}\}$ NMR (dmf- d_7), δ (ppm): 214.8 (d, $^2J(\text{C},\text{P}) = 10.8$ Hz, CO), 213.8 (d, $^2J(\text{C},\text{P}) = 10.8$ Hz, CO), 210.7 (br s, CO), 209.8 (d, $^2J(\text{C},\text{P}) = 28.7$ Hz, CO). $^{31}\text{P}\{^1\text{H}\}$ NMR (dmf- d_7), δ (ppm): 49.5 (m, 1 P), -9.3 (m, 1 P), -24.2 (m, 1 P), -54.7 (m, 1 P), -71.3 (m, 1 P), -106.2 (m, 1 P), -116.0 (m, 1 P).

Preparation of $[\text{K}(2,2,2\text{-crypt})]_2[\eta^2\text{-(CH}_2\text{Ph)P}_7\text{W}(\text{CO})_4]\cdot\text{en}$. Method A. In a vial in a drybox, K_3P_7 (29.6 mg, 0.089 mmol), 2,2,2-crypt (100.0 mg, 0.27 mmol) and $(\text{C}_6\text{H}_3\text{Me}_3)\text{W}(\text{CO})_3$ (34.4 mg, 0.089 mmol) were combined in en (~ 3 mL) and stirred for 12 h producing a red solution. Solid $(\text{PhCH}_2)\text{Me}_3\text{NBr}$ (20.5 mg, 0.089 mmol) was added and the reaction mixture stirred for an additional 12 h yielding a maroon solution. The reaction mixture was transferred from the vial to a 25 mL Schlenk flask, and the head gases were removed under vacuum. The Schlenk flask was then backfilled with CO (~ 1 atm) and the flask left open to the bubbler with a flow of CO for 30 s. The reaction mixture was vigorously stirred under a CO atmosphere for 12 h, producing a yellow solution and yellow powder. The mother liquor was removed, yielding a yellow powder that was washed with tol and dried under vacuum (powder yield, 81 mg, 61%).

Method B. $[\text{K}(2,2,2\text{-crypt})]_3[\eta^2\text{-P}_7\text{W}(\text{CO})_4]\cdot\text{en}$ (0.089 mmol) was prepared as described above (Method A). Solid $(\text{PhCH}_2)\text{Me}_3\text{NBr}$ (20.5 mg, 0.089 mmol) was added to the solution and the reaction mixture stirred for 8 h. ^{31}P NMR spectroscopic analysis of the mother liquor showed quantitative conversion to **3c**. Anal. Calcd for $\text{C}_{49}\text{H}_{88}\text{N}_6\text{O}_{16}\text{K}_2\text{P}_7\text{W}$: C, 39.34; H, 5.93; N, 5.62. Found: C, 38.50; H, 5.69; N, 5.44. IR data (KBr pellet), cm^{-1} : 1964 (s), 1840 (s), 1824 (s), 1774 (s). ^1H NMR (dmf- d_7), δ (ppm): 7.3-7.0 (m, CH_2Ph), 1.83, 1.53 (CH_2Ph). $^{13}\text{C}\{^1\text{H}\}$ NMR (dmf- d_7), δ (ppm): 215 (m, CO), 214 (m, CO), 211 (br s, CO), 210 (d, $^2J(\text{C},\text{P}) = 30$ Hz, CO), 143.8 (br s, ipso C), 130, 128, 125 (CH_2Ph), 26.9 (d, $^1J(\text{C},\text{P}) = 30$ Hz, CH_2Ph). $^{31}\text{P}\{^1\text{H}\}$ NMR (dmf- d_7), δ (ppm): 120 (m, 1 P), -1 (m, 1 P), -38 (m, 1 P), -58 (m, 1 P), -80 (m, 1 P), -119 (m, 2 P).

Reaction of $[\eta^4\text{-P}_7\text{W}(\text{CO})_3]^{3-}$ and " $\text{Mo}(\text{CO})_3$ ". In vial 1 in a drybox, K_3P_7 (29.6 mg, 0.089 mmol), 2,2,2-crypt (100.0 mg, 0.27 mmol), and $(\text{C}_6\text{H}_3\text{Me}_3)\text{W}(\text{CO})_3$ (34.4 mg, 0.089 mmol) were dissolved in en (~ 3 mL) and stirred for 12 h producing a red solution. In vial 2, $(\text{C}_7\text{H}_8)\text{Mo}(\text{CO})_3$ (24.1 mg, 0.089 mmol) was suspended in toluene (~ 1 mL) and then added dropwise to the contents of vial 1. The mixture was stirred for 2 h without a change in the red color of the solution. After 24 h, the reaction vessel contained golden yellow crystals that were removed from the mother liquor, washed with toluene, and dried under vacuum (crystalline yield, 46 mg). A crystal of $[\text{K}(2,2,2\text{-crypt})]_2[\eta^2\text{-HP}_7\text{W}(\text{CO})_4]\cdot\text{en}$ was selected for single-crystal X-ray diffraction study. IR and ^{31}P NMR spectroscopic analysis of

the crystals revealed **5a** and **5b** in a 10:1 ratio. Visual inspection of the crystals also showed five that were red in color. Single crystal X-ray diffraction revealed a "K–Mo–P" compound with a BaVS₃-type structure.³⁰

Attempts at Deprotonation. Solutions of $[\eta^2\text{-HP}_7\text{M}(\text{CO})_4]^{2-}$ (M = Mo, W) (0.089 mmol) were prepared in Schlenk flasks as described above (Method A for **5a**). Solid NaOMe (7.2 mg, 0.134 mmol) or solid H₂N(CH₂)₂NHLi (8.9 mg, 0.134 mmol) were added and the reaction mixtures stirred for 8 h. The products were then assayed by ³¹P NMR spectroscopy.

X-ray Crystallographic Studies. **[K(2,2,2-crypt)]₂[η²-HP₇W(CO)₄]**·en.** A yellow colored crystal with dimensions 0.50 × 0.20 × 0.20 mm was placed on the Enraf-Nonius CAD-4 diffractometer. The crystal's final cell parameters and crystal orientation matrix were determined from 25 reflections in the range 18.1 < 2θ < 33.5°; these constants were confirmed with axial photographs. Data were collected [MoK_α] with ω/2θ scans over the range 2.0–22.5° with a scan width of (0.90 + 0.35 tan θ)° and a variable scan speed of 2.06–4.12° min⁻¹ with each scan recorded in 96 steps with the outermost 16 steps on each end of the scan being used for background measurement. Three ψ-scan reflections were collected twice over the range 8.1 < θ < 13.0°; the absorption correction was applied with transmission factors ranging from 0.8086 to 0.9994 with an average correction of 0.9315.**

Data were corrected for Lorentz and polarization factors and absorption and reduced to observed structure-factor amplitudes using the program package NRCVAX. Systematic absences indicated the centrosymmetric space group C2/c (No. 15) or the noncentrosymmetric space group Cc (No. 9). Intensity statistics were inconclusive although slightly favoring the acentric case. The structure was determined with the successful location of the tungsten and seven phosphorus atoms using SHELXS-86 in the acentric space group Cc. Subsequent difference-Fourier maps revealed the location of all remaining non-hydrogen atoms within the molecule and two K·crypt ligands. Cor-

relation coefficients indicated that the atoms comprising the main molecule were strongly influencing one another, indicating that the true space group was C2/c. SHELXL was used to refine the structure, based upon F_o² and σ(F_o²). The function minimized during the full-matrix least-squares refinement was Σw(F_o² - F_c²) where w = 1/[σ²(F_o²) + (0.0869P)²] and P = (max(F_o², 0) + 2F_c²)/3. Hydrogen atoms were placed in calculated positions but not refined. A final difference-Fourier map was featureless with |Δρ| ≤ 0.673 e Å⁻³.

[K(2,2,2-crypt)]₂[η²-HP₇Mo(CO)₄]·en.** A procedure identical to that described above was used for the isomorphous [K(2,2,2-crypt)]₂[η²-HP₇Mo(CO)₄]**·en** complex. Data were collected [MoK_α] with ω/2θ scans over the range 2.4–22.5°. The data were not corrected for absorption or decay. The structure was determined with isomorphous replacement based upon a previous [K(2,2,2-crypt)]₂[η²-HP₇Mo(CO)₄]**·en** study. The final difference-Fourier map was featureless with |Δρ| ≤ 0.848 e Å⁻³.**

Acknowledgment. This work was funded by the National Science Foundation through Grant CHE-9500686. We gratefully acknowledge Prof. Rinaldo Poli for helpful discussions.

Supporting Information Available: A complete listing of crystallographic data positional parameters, thermal parameters, bond distances and angles, a table showing the conversion from the text numbering scheme to that used in the Supporting Information, and ORTEP diagrams of the anions showing the numbering scheme used in the Supporting Information for [K(2,2,2-crypt)]₂[η²-HP₇M(CO)₄] where M = Mo, W (23 pages). This material is contained in many libraries on microfiche, immediately follows this article in the microfilm version of the journal, and can be ordered from the ACS; see any current masthead page for ordering information.

IC9511534